# Structural Analysis of a Metallosupramolecular Polyelectrolyte – Amphiphile Complex at the Air/Water Interface

**Pit Lehmann, Dirk G. Kurth,* Gerald Brezesinski, and Christian Symietz[a]**

**Abstract:** A detailed analysis of a metallosupramolecular coordination polyelectrolyte – amphiphile complex (PAC) at the air/water interface is presented based on Langmuir isotherm measurements, Brewster angle microscopy as well as X-ray reflectance and diffraction measurements. The PAC is prepared in solution by metal-ion coordination of $Fe(OAc)_2$ and 1,4-bis(2,2′:6′,2″-terpyridin-4′-yl)benzene followed by self-assembly with dihexadecyl phosphate (DHP). The spreading of the PAC at the air/water interface results in a Langmuir film with a stratified architecture, such that DHP forms a monolayer on the water surface, while the metallosupramolecular coordination polyelectrolyte (MEPE) is immersed in the aqueous subphase. Electrostatic interactions of MEPE and DHP force the alkyl chains into an upright, hexagonal lattice even at low surface pressures. This work illustrates how supramolecular, colloidal, and surface chemistry can be combined to create complex architectures with tailored characteristics that may *not* be accessible through self-organization in the liquid phase.

**Keywords:** amphiphiles · coordination chemistry · polyelectrolytes · supramolecular chemistry · surface chemistry

## Introduction

The availability of amphiphiles and polyelectrolytes, the ease of formation, and the wide range of possible structures and characteristics make polyelectrolyte – amphiphile complexes (PACs) materials of general interest in fundamental research and technological applications. The formation of these materials results from the spontaneous assembly of amphiphiles and polyelectrolytes, driven by cooperative electrostatic and hydrophobic interactions. The intrinsic properties of amphiphiles to self-assemble in combination with the topography of the macromolecular backbone give rise to highly ordered, extended equilibrium architectures.[1–5] The prospect of integrating molecular devices into either one of the constituents of the PAC bears promising potential towards the engineering of functional materials. The modularity of this approach assures versatility in terms of available components, provides extensive control of function and structure, and permits building of architectures with structures of several different sizes.

With the recent discovery of metallosupramolecular coordination polyelectrolytes (MEPE),[6] novel components are now available that allow a facile entry to advanced PACs.[7] Metallosupramolecular devices possess diverse reactive, kinetic, and thermodynamic properties that make them attractive for applications in electronic, magnetic, and photonic materials. The combination of metallosupramolecular devices as the functional and amphiphiles as the structural component, respectively, provides an attractive route to customize particular properties, including solubility and surface activity, as well as to fabricate multi-component composite materials.

There are several approaches to prepare extended assemblies of metallosupramolecular devices, including thin films and monolayers on planar[8, 9] and colloidal interfaces,[10] as well as liquid crystalline phases.[11] Amphiphilic and water-insoluble coordination arrays and polymers can be spread at the air/water interface.[12–14] The well-defined conditions at the air/water interface are attractive for the synthesis of highly ordered non-equilibrium architectures by Langmuir – Blodgett (LB) transfer, which are generally not accessible through self-assembly in the liquid phase. The air/water interface is also ideal for the investigation of interactions between polyelectrolytes and amphiphiles. In general, water-soluble polyelectrolytes are adsorbed from the subphase to an amphiphilic monolayer. The PAC, which is formed at the air/water interface, can subsequently be transferred onto a solid support. This concept can be used to stabilize amphiphilic membranes in analogy to the cytoskeleton and serves as a model system for charged interfaces.[15–19]

In contrast to these methods, the approach presented herein relies on a preformed PAC; that is, the PAC is self-assembled in solution and isolated prior to distribution at the air/water interface. First, MEPE (**1**) is prepared in aqueous solution by self-assembly of ditopic 1,4-bis(2,2′:6′,2″-terpyridin-4′-yl)ben-

[a] D. G. Kurth, Dr. P. Lehmann,
Dr. G. Brezesinski, Dipl.-Phys. C. Symietz
Max-Planck-Institute of Colloids and Interfaces
14424 Potsdam (Germany)
Fax: (+49) 0331-567-9202
E-mail: kurth@mpikg-golm.mpg.de



0947-6539/01/0708-1646 $ 17.50+.50/0

zene and suitable metal ions, such as $Fe^{II}$ (see Figure 1).[6] With most transition metal ions, terpyridines form stereochemically non-ambiguous complexes with pseudo-octahedral coordination geometry ($D_{2d}$ symmetry).[20] Therefore, metal-ion coordination of bis-terpyridine ligands results in linear, extended, positively charged macromolecules. Subsequent self-assembly of MEPE (**1**) and the amphiphile dihexadecyl phosphate (DHP) results in a completely non-covalent, hydrophobic PAC (**2**).[7] It should be noted that, under these experimental conditions, the composition of PAC (**2**) shows six amphiphiles per repeating unit, which is defined as one ditopic ligand along with one metal ion. Two DHPs can form a bond through electrostatic interactions of the charged components, while the remaining four DHPs can bond to each other through hydrophobic and hydrogen-bonding interactions. This particular non-stoichiometric charge-to-amphiphile ratio is not uncommon in PACs.[21] The solubility of PAC (**2**) in common organic solvents indicates that the amphiphiles efficiently shield the hydrophilic portion of MEPE (**1**). We therefore assume that, in solution, the amphiphiles are predominately located around the hydrophilic metal-ion centers as depicted in Figure 1.

As we showed recently, PAC (**2**) spreads at the air/water interface, and the resulting Langmuir monolayer can be transferred onto solid supports resulting in highly organized, anisotropic Y-type LB multilayers.[7] The characteristic metal-to-ligand charge transfer band observed in LB multilayers demonstrates that the MEPE (**1**) is present in the PAC (**2**) monolayer at the air/water interface. However, the exact structure of the PAC (**2**) monolayer at the air/water interface has not been addressed to date.

The present study was undertaken to gain detailed insight into the structure of a preformed PAC monolayer at the air/water interface, which is of paramount importance for the understanding of the interaction between MEPE and amphiphiles as well as the principal parameters that determine the final LB film architecture.

**Abstract in German:** *In einer detaillierten Studie berichten wir über die Struktur eines metallo-supramolekularen Koordinations-Polyelektrolyt–Amphiphil-Komplexes (PAC) an der Wasser/Luft Grenzfläche. Der PAC entsteht in Lösung durch Metallionen-Koordination von $Fe(OAc)_2$ und 1,4-bis(2,2′:6′,2″-terpyridin-4′-yl)benzol gefolgt von Selbstorganisation mit Dihexadecylphosphat (DHP). Die Ergebnisse der Langmuir Isothermen, Brewster-Winkel-Mikroskopie, sowie Röntgen Reflexion und Beugung zeigen übereinstimmend, daß der PAC an der Wasser/Luft Grenzfläche eine Langmuir-Monolage mit einer geschichteten Architektur ausbildet. Die DHP-Moleküle bilden eine partiell geladene Monolage auf der Wasseroberfläche, an die der metallo-supramolekulare Koordinations-Polyelektrolyt von unten anbindet. Elektrostatische Wechselwirkungen zwischen der MEPE und DHP Schicht zwingen die Alkylketten in ein aufrechtes, hexagonales Gitter selbst bei kleinen Oberflächendrücken. Diese interdisziplinäre Arbeit zeigt, wie die Supramolekulare Chemie, die Kolloidwissenschaften und die Grenzflächenforschung mit einander kombiniert werden können, um komplexe Architekturen mit maßgeschneiderten Strukturen und Eigenschaften aufzubauen, die nicht ohne weiteres in der Volumenphase durch Selbstorganisation entstehen.*

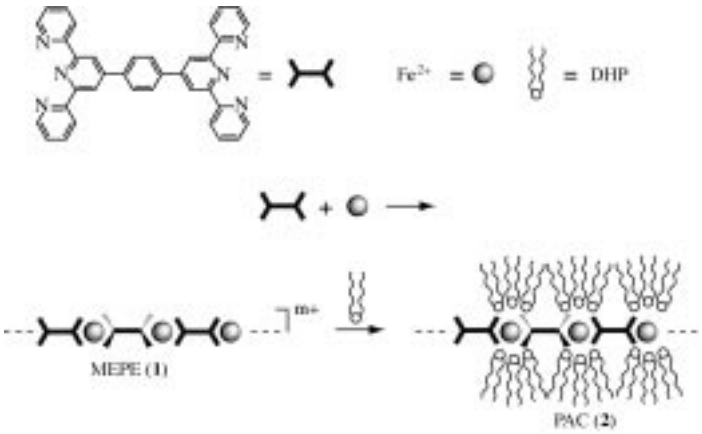


Figure 1. Self-assembly of the polyelectrolyte–amphiphile complex PAC (**2**). The octahedral coordination geometry around the metal ion is indicated by the dotted and solid wedges.

## Results and Discussion

**Langmuir isotherms**: The PAC (**2**) pressure–area isotherm, which is very reproducible, is shown in Figure 2. In contrast to our previously published results,[7] the molecular area of the isotherm was calculated with a molecular mass of PAC (**2**) in agreement with a composition of six amphiphiles per MEPE repeating unit.[22] The PAC (**2**) monolayer collapses at a remarkably high pressure of 62 $mN\,m^{-1}$. The area at the collapse is 1.9 $nm^2$ per repeating unit. Upon expansion, a slight hysteresis is observed. In contrast to neat DHP (inset), the PAC (**2**) isotherm shows no distinct phase transition between the tilted and untilted liquid condensed phase. The lack of a liquid expanded phase and the steep slope of the lateral pressure in the isotherm of neat DHP is typical for long-chain amphiphiles with strong van der Waals attractions.

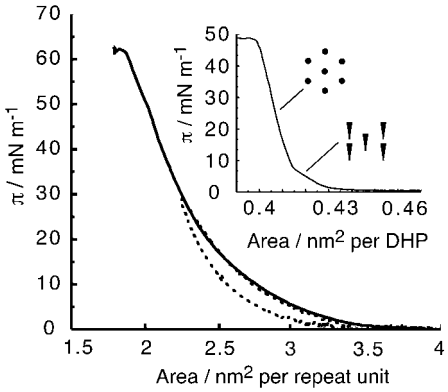


Figure 2. Compression isotherm (solid line) and expansion hysteresis (dotted line) of the PAC (**2**) monolayer at the air/water interface. The monolayer of neat DHP (inset) shows a distinct phase transition. The structure of the alkyl chains in both phases is schematically depicted.

Molecular modeling suggests the following approximate dimensions of a MEPE (**1**) repeating unit: the width is 1.15 (±0.1) nm and the metal ion–metal ion distance is 1.55 (±0.1) nm.[23] If packing effects are neglected, the area of a single repeating unit with the longitudinal axis oriented parallel to the interface is approximately 1.8 nm$^2$. DHP, on the other hand, occupies an area of 0.4 nm$^2$ (see inset in Figure 2 and Table 1). The area at the collapse pressure corresponds approximately to a single MEPE (**1**) repeating unit *or* five DHP molecules. We propose that the Langmuir monolayer has a stratified bilayer architecture, in which the top consists of DHP molecules and the bottom consists of MEPE (**1**). The verification of this hypothesis and the fact that the actual collapse area (1.9 nm$^2$) is smaller than the spatial requirement of the six DHP molecules (2.4 nm$^2$), which belong to a single repeating unit, will be discussed in the following sections.

Table 1. Unit cell parameters $a$, $b$, and $\gamma$, tilt angle $t$, cross-sectional area $A_0$, and positional correlation length, $\xi$, of alkyl chains in (**a**) PAC (**2**) and (**b**) neat DHP monolayers as derived from grazing incidence X-ray diffraction.

| **a** PAC (**2**) | | | | | | | |
|---|---|---|---|---|---|---|---|
| $p$ [mN m$^{-1}$] | $a$ [Å] | $b$ [Å] | $\gamma$ [deg] | $t$ [deg] | $A_0$ [Å$^2$] | $\xi_1$ [Å] | $\xi_2$[a] [Å] |
| 5 | 4.81 | 4.81 | 120.0 | 0.5 | 20.1 | 105 | – |
| 10 | 4.80 | 4.80 | 120.0 | 0 | 20.0 | 82 | – |
| 20 | 4.77 | 4.83 | 119.6 | 0 | 20.1 | 120 | 40 |
| 40 | 4.75 | 4.83 | 119.5 | 0 | 20.0 | 85 | 42 |
| **b** DHP | | | | | | | |
| $p$ [mN m$^{-1}$] | $a$ [Å] | $b$ [Å] | $\gamma$ [deg] | $t$ [deg] | $A_0$ [Å$^2$] | $\xi_1$ [Å] | $\xi_2$[a] [Å] |
| 2 | 4.90 | 4.86 | 120.2 | 11.3 | 20.2 | 167 | 78 |
| 5 | 4.86 | 4.85 | 120.1 | 9.7 | 20.1 | 167 | 69 |
| 10 | 4.82 | 4.82 | 120.0 | 0.8 | 20.0 | 167 | – |
| 20 | 4.80 | 4.80 | 120.0 | 0 | 20.0 | 186 | – |

[a] In a hexagonal lattice $\xi_1 = \xi_2$.

**Brewster angle microscopy**: Representative Brewster angle microscopy (BAM) images that reveal the morphology of the PAC (**2**) monolayer at different lateral pressures are shown in Figure 3. At zero surface pressure, large elongated domains are observed. These domains fuse upon compression and a condensed film is observed at surface pressures exceeding 10 mN m$^{-1}$. Upon expansion of the monolayer, the individual domains reappear under retention of their characteristic elongated shape.

Furthermore, bright spots are visible on both BAM images. The spots occur immediately after spreading; that is, they are present at zero surface pressure and do not develop during compression. The high reflectance of these spots indicates that they are comprised of three-dimensional structures. The dimensions of the aggregates are probably much smaller than suggested by BAM images.[24] This assumption is supported by the fact that the aggregates do not contribute significantly to the reflectance of the interface as demonstrated by X-ray reflectivity (see below). The aggregates reduce the area of the monolayer at all pressures and are responsible for the above-mentioned reduced collapse area of the PAC (**2**) monolayer. The collapse area (1.9 nm$^2$) corresponds more closely to five (out of six) DHP molecules (0.4 nm$^2$ per DHP molecule). To

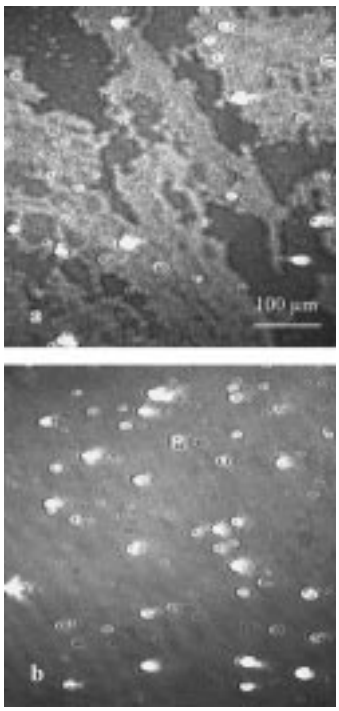


Figure 3. The morphology of PAC (**2**) monolayers at a) 0 mN m$^{-1}$ and b) 10 mN m$^{-1}$ as seen with BAM.

conform to the steric requirement of one MEPE (**1**) repeating unit (1.8 nm$^2$), some DHP molecules aggregate. There is no evidence for crystalline bulk material as shown by X-ray diffraction measurements (see below). This means that the aggregates are amorphous and/or too small to provide sufficient diffraction intensity.

In contrast to PAC (**2**) monolayers, neat DHP forms a homogeneous monolayer at surface pressures exceeding 10 mN m$^{-1}$ with no evidence for three-dimensional aggregates. In addition, the domains in DHP monolayers are of uncharacteristic shape and size. The occurrence of elongated domains in PAC (**2**) monolayers is therefore attributed to the particular interactions between DHP and MEPE (**1**) at the air/water interface.

**X-ray reflectivity**: In order to provide further support for the hypothesis of a stratified bilayer architecture of the PAC (**2**) monolayer, the X-ray reflectivity (XRR) of the interface was determined. Figure 4 shows XRR curves (open circles) of the PAC (**2**) monolayer for different lateral pressures, as well as computed reflectance profiles (solid lines). The fits are in good agreement with the experimental data. From the occurrence of the Kiessig interference fringes in the reflectance profiles, we conclude that the PAC (**2**) monolayer is homogeneous in thickness and composition.[25] The above-mentioned three-dimensional aggregates of DHP are either too small and/or too few to affect the reflectance of the interface significantly. The film thickness in the investigated pressure range does not change significantly as indicated by the almost constant spacing of the Kiessig fringes. The total thickness of the Langmuir monolayer amounts to 3.2 nm at 10 mN m$^{-1}$, 3.23 nm at 20 mN m$^{-1}$ and 3.25 nm at 40 mN m$^{-1}$, respectively.



0947-6539/01/0708-1648 $ 17.50+.50/0 *Chem. Eur. J.* **2001**, *7*, No. 8

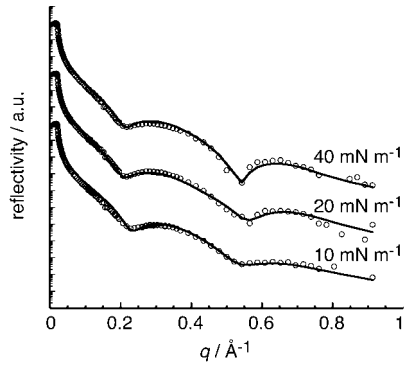


Figure 4. Experimental X-ray reflectance curves of the PAC (**2**) monolayer (open circles) at the air/water interface at different surface pressures as a function of the wave vector $q$. (The curves are shifted in $y$ direction for clarity). The details of the electron density profile, used for these fits, are shown in Figure 5.

The computed reflectivity curves are based on a stratified interface that consists of three layers, each one with a uniform electron density, $\rho_{el}$, thickness and interfacial roughness, $\tau$. The interfacial roughness is introduced to allow a smooth transition between each interface. A representative electron density profile of the PAC (**2**) monolayer at a surface pressure of 20 mN m$^{-1}$ is shown in Figure 5.

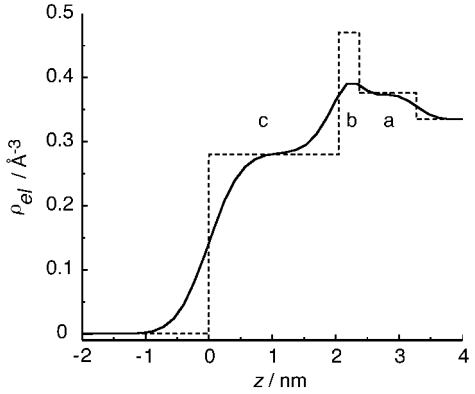


Figure 5. Representative example of the computed electron density profile perpendicular to the interface of the PAC (**2**) monolayer (solid line) at 20 mN m$^{-1}$. The dotted line illustrates thickness and electron density of each stratum of the three-layer model. The solid line takes into account the interfacial roughness. Bulk water is on the right at large $z$ values. The MEPE (**1**) layer has a thickness of 0.9 nm (**a**). The phosphate head groups of DHP constitute the middle layer (**b**, 0.28 nm) and the alkyl chains of DHP terminate the monolayer at the top (**c**, 2.05 nm). Further details are given in the text.

The fit can be interpreted as follows: starting from the water subphase, box **a** of intermediate electron density ($\rho_{el}$ 0.376 Å$^{-3}$) and a thickness of 0.9 nm ($\tau = 0.18$ nm) corresponds to MEPE (**1**) immersed in the aqueous subphase. The volume fraction of MEPE (**1**) in the aqueous subphase corresponds to 35 %.[26] With an electron density, $\rho_{el}$, of 0.47 Å$^{-3}$ for MEPE (**1**) and 0.33 Å$^{-3}$ for water, the theoretical electron density of this box amounts to 0.38 Å$^{-3}$, which is in agreement with the experimental value. The increased electron density, compared with that of pure water, is an indication for the presence of MEPE (**1**) at the water surface. Box **b** of high electron density ($\rho_{el} = 0.47$ Å$^{-3}$) and a thickness of 0.28 nm ($\tau = 0.35$ nm) is attributed to the phosphate head groups of DHP. Neglecting the presence of water molecules in this layer, the thickness and electron density are expected to be approximately 0.26 nm and 0.48 Å$^{-3}$, respectively, which is, within the simplified structural model, in agreement with the experimental values. Finally, box $c$ of low electron density ($\rho_{el} = 0.28$ Å$^{-3}$) and a thickness of 2.05 nm ($\tau = 0.4$ nm) is ascribed to the alkyl chains of DHP. The values are in agreement with a layer of untilted $C_{16}$-alkyl chains in all-*trans* configuration. The XRR data confirm the hypothesis of a stratified monolayer architecture. The amphiphilic component forms a close packed stratum (with occasional aggregates) with the phosphate head groups pointing into the water surface coupled to the layer of MEPE (**1**), which is immersed in the subphase (see Figure 6).

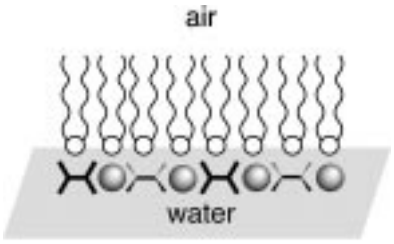


Figure 6. Schematic bilayer architecture of the PAC (**2**) monolayer at the air/water interface. The amphiphilic component of the PAC forms a (partially) charged template layer, to which MEPE (**1**) adsorbs from underneath.

**Grazing incidence X-ray diffraction**: The occurrence of crystalline order within the PAC (**2**) monolayer was investigated with grazing incidence X-ray diffraction (GID). The data are shown in Figure 7, and the corresponding unit cell values are presented in Table 1. For the PAC (**2**) monolayer, we observe at surface pressures of 5 and 10 mN m$^{-1}$ one diffraction peak at $q_z = 0$, which is characteristic of hexagonally packed, untilted alkyl chains. From the peak extension into the $q_z$ direction, the scattering length, $l$, of the molecules is calculated to be 2.24 nm, corresponding to an all-*trans* $C_{16}$-alkyl chain and the ether linkage to the phosphate head group. At surface pressures of 20 mN m$^{-1}$ and 40 mN m$^{-1}$, the Bragg peaks could only be fitted with two Lorentzian functions at different $q_{xy}$ ($q_z = 0$) positions, in accordance with a rectangular packing of untilted alkyl chains (see Figure 7). The distortion of the lattice along the nearest neighbor (NN) direction increases with increasing surface pressure. While the GID measurements provide proof for crystalline order within the alkyl chains of the DHP stratum, there is no direct evidence for long-range order in the MEPE (**1**) underneath the DHP layer, presumably because the polyelectrolyte is disordered.

In the following paragraph, we will discuss the structure of neat DHP monolayers. At low surface pressures of 2 mN m$^{-1}$ and 5 mN m$^{-1}$, the DHP alkyl chains form a rectangular lattice with the alkyl chains tilting towards the nearest neighbor (NN). The $q_z$ positions of the Bragg peaks are $q_z = 0$ and $q_z =$

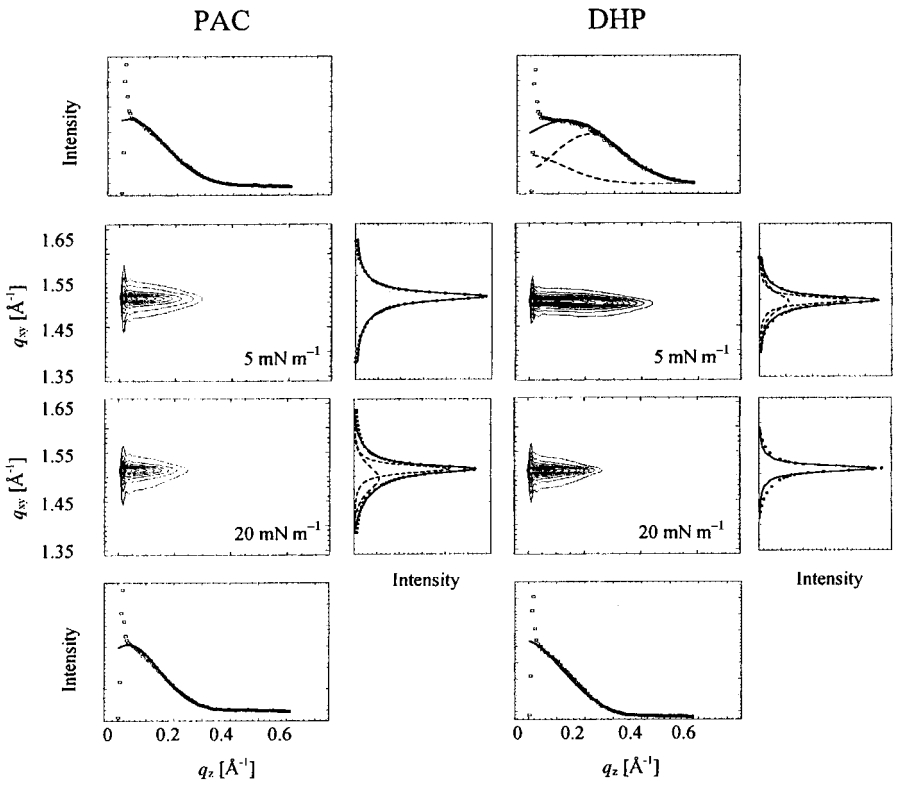


Figure 7. Contour plots of the X-ray intensities of the scattering vector $q$ as a function of the in-plane component $q_{xy}$ and the vertical component $q_z$ of the polyelectrolyte–amphiphile complex (PAC (**2**)) and dihexadecyl phosphate (DHP). The plots show the data (squares) and the individual fits (solid line) of the Bragg peaks and Bragg rods.

0.26 Å$^{-1}$ (2 mN m$^{-1}$) and $q_z = 0$ and $q_z = 0.22$ Å$^{-1}$ (5 mN m$^{-1}$), respectively. At a surface pressure of 10 mN m$^{-1}$ and 20 mN m$^{-1}$, the alkyl chains form a hexagonal lattice with untilted chains, and only one diffraction peak at $q_z = 0$ is observed. In the tilted liquid–condensed phase, the projected molecular area, $A_{xy}$, is a linear function of the surface pressure $p$. The dependence can be described by Equation (1), where $K_1$ and $K_2$ are arbitrary constants.

$$A_{xy} = K_1 - K_2 p \quad (1)$$

As can be seen in Table 1b, the cross-sectional area $A_0 = A_{xy}\cos(t)$, where $t$ is the tilt angle of the alkyl chains, does not depend on the surface pressure ($A_0 \sim 20.1$ Å$^2$). Therefore, $1/\cos(t)$ is a linear function of the surface pressure. The initially tilted alkyl chains are in an upright orientation if the surface pressure exceeds 10.2 mN m$^{-1}$. The scattering length, $l$, of the molecules is 2.32 nm. The values for the length of DHP determined in different samples (PAC, DHP) and methods (XRR, GID) are consistent and confirm the assignments made in the XRR section.

In comparison to neat DHP monolayers, the structure of the amphiphiles is affected in two significant ways by coupling to MEPE (**1**) in the aqueous subphase. In the neat DHP monolayer, the alkyl chains are in a tilted, rectangular lattice at low surface pressure. Compression results in an untilted hexagonal lattice. In contrast, we observe an untilted, hexagonal lattice in the PAC (**2**) monolayer at low surface pressures (< 10 mN m$^{-1}$). We assume that, in the PAC (**2**) monolayer, electrostatic interactions between MEPE (**1**) and DHP force the alkyl chains into a hexagonal, untilted lattice at low surface pressures. The alkyl chains remain untilted at higher surface pressures (> 20 mN m$^{-1}$), but the lattice distorts from hexagonal to rectangular. In addition, the positional correlation lengths (Table 1) are smaller in the PAC (**2**) monolayer compared to neat DHP, because of a slight mismatch of the steric requirement of the MEPE (**1**) repeating unit (length 1.55 nm) and the DHP molecules (diameter 0.5 nm per alkyl chain).

## Summary

Spreading of the preformed PAC (**2**) at the air/water interface results in a Langmuir monolayer with a stratified bilayer architecture. The amphiphilic molecules assemble into a closed packed monolayer (with occasional aggregates) on the water surface, while the MEPE (**1**) is immersed in the aqueous subphase and is electrostatically coupled to the monolayer, as schematically shown in Figure 6. The structural flexibility required to form this stratified architecture is provided by the non-covalent interactions within the PAC assembly.

The interactions between DHP and MEPE (**1**) evoke an untilted hexagonal liquid–condensed phase of the aliphatic alkyl chains, even at low surface pressures. The electrostatic coupling is responsible for the stability of the Langmuir monolayer and its high collapse pressure. In contrast to the Langmuir monolayer of neat DHP, the polycrystalline nature of the PAC (**2**) Langmuir monolayer explains the absence of phase transitions upon compression.

The driving force for the structural organization of the preformed PAC (**2**) is provided by the prevailing surface tension across the air/water interface.[27] As was recently shown,[7] the stratified bilayer architecture of the Langmuir film evokes LB films with Y-type architecture if the monolayer is transferred on solid supports. This Y-type architecture of the LB films strongly supports the proposed structure model of the Langmuir monolayer. Ongoing experiments in our laboratory suggest that this method is of general utility to customize the surface chemical properties of metallosupramolecular coordination polyelectrolytes. Full answers to the types of bulk phases, liquid crystalline and lyotropic phases formed by these PACs require further experimental and theoretical efforts.



0947-6539/01/0708-1650 $ 17.50+.50/0 *Chem. Eur. J.* **2001**, *7*, No. 8

## Experimental Section

The MEPE (**1**) and the PAC (**2**) were synthesized according to previously published procedures.[6, 7]

The pressure/area isotherms were measured with a Lauda FW 2 film balance (Lauda GmbH, Königshofen, Germany). The PAC (**2**) (2.45 mg) was dissolved in chloroform (10 mL). The solution (300 μL) was spread onto distilled water (Milli-Q water with a resistivity exceeding 18.2 MΩ cm) at 20 °C.

Brewster angle microscopy images were taken with a Brewster angle microscope (BAM 2, Nanofilm Technology GmbH, Göttingen, Germany, 20 mW Laser, wavelength 514 nm, resolution 3 μm), and a Riegler&Kirstein film balance (R&K, Wiesbaden, Germany).

Synchrotron X-ray experiments at the air/water interface were performed at the undulator beamline BW1 at HASYLAB, DESY (Hamburg, Germany).[28] The Synchrotron beam was made monochromatic by Bragg reflection at a beryllium (002) crystal. The X-ray reflectivity data were analyzed with a computer program.[29] A box model was applied. The reflectivity of the interface was calculated according to classical electrodynamic theory as a function of the scattering vector $q_z = (4\pi \sin\alpha_i)/\lambda$, where $\alpha_i$ is the angle of incidence and $\lambda$ is the X-ray wavelength ($\approx 1.36$ Å).

GID experiments were carried out with an angle of incidence of $\alpha_i = 0.85\alpha_c$, with $\alpha_c$ being the critical angle of total external reflection of water (0.138°). A detailed description of the method is given elsewhere.[30, 31] The scattered intensity was detected with a position-sensitive detector as a function of the vertical component of the scattering vector $q_z = (2\pi/\lambda)\sin\alpha_f$, where $\alpha_f$ is the angle of diffraction in the plane of incidence. The in-plane scattering component (with respect to the interface) $q_{xy} = (4\pi/\lambda)\sin\Theta_{xy}$ was detected by scanning over the range along the horizon, where $2\Theta_{xy}$ is the angle between the incident and the diffracted beam projected onto the horizontal plane. The data were analysed as follows: contour plots of the corrected X-ray intensities as a function of $q_{xy}$ and $q_z$ gave a first indication of the order of the assembled molecules and the lattice type. Integration of the scattered intensity $q_{xy}$ ($q_z$) over the $q_z$ ($q_{xy}$) range reveal the Bragg peaks (rods), which were fitted with Lorentzian (peaks) or Gaussian (rods) profiles. The scattering length, $l$, of the molecules was calculated from the full width at half maximum (*FWHM*) of the Bragg rod, according to $l = 2\pi/FWHM$ and the positional correlation length $\xi$ from the Bragg peak $\Delta_{int}(q_{xy})$ (corrected for resolution effects of the detector) according to $\xi = 2/\Delta_{int}(q_{xy})$.

## Acknowledgement

The authors thank Helmuth Möhwald for inspiring discussions, and Markus Schütte and Christa Stolle for the preparation of the compounds. We thank HASYLAB at DESY, Hamburg, Germany, for beam time, and Kristian Kjaer for his help in setting up the X-ray experiment.

[1] M. Antonietti, C. Göltner, *Angew. Chem.* **1997**, *109*, 944 – 964; *Angew. Chem. Int. Ed. Engl.* **1997**, *36*, 910 – 929.
[2] C. K. Ober, G. Wegner, *Adv. Mater.* **1997**, *9*, 17 – 31.
[3] W. J. MacKnight, E. A. Ponomarenko, D. A. Tirrell, *Acc. Chem. Res.* **1998**, *31*, 781 – 788.
[4] S. Zhou, B. Chu, *Adv. Mater.* **2000**, *12*, 545 – 556.
[5] M. Antonietti, A. Thünemann, *Curr. Opin. Colloid Interface Sci.* **1996**, *1*, 667 – 671.
[6] M. Schütte, D. G. Kurth, M. Linford, H. Cölfen, H. Möhwald, *Angew. Chem.* **1998**, *110*, 3058 – 3061; *Angew. Chem. Int. Ed.* **1998**, *37*, 2891 – 2894.
[7] D. G. Kurth, P. Lehmann, M. Schütte, *Proc. Natl. Acad. Sci. USA* **2000**, *97*, 5704 – 5707.
[8] D. G. Kurth, R. E. Osterhout, *Langmuir* **1999**, *15*, 4842 – 4846.
[9] a) T. Salditt, Q. R. An, A. Plech, J. Peisl, C. Eschbaumer, C. H. Weidl, U. S. Schubert, *Thin Solid Films* **1999**, *354*, 208 – 214; b) A. Semenov, J. P. Spatz, M. Moller, J.-M. Lehn, B. Sell, D. Schubert, C. H. Weidl, U. S. Schubert, *Angew. Chem.* **1999**, *111*, 2701 – 2705; *Angew. Chem. Int. Ed.* **1999**, *38*, 2547 – 2550.
[10] a) D. G. Kurth, F. Caruso, C. Schüler, *Chem. Commun.* **1999**, 1579 – 1580; b) F. Caruso, C. Schüler, D. G. Kurth, *Chem. Mater.* **1999**, *11*, 3394 – 3399.
[11] D. W. Bruce, in *Inorganic Materials* (Eds.: D. W. Bruce, D. O'Hare), 2nd ed., Chapter 8, Wiley, New York, **1996**.
[12] a) I. Weissbuch, P. N. W. Baxter, S. Cohen, H. Cohen, K. Kjaer, P. B. Howes, J. Als-Nielsen, G. S. Hanan, U. S. Schubert, J.-M. Lehn, L. Leiserowitz, M. Lahav, *J. Am. Chem. Soc.* **1998**, *120*, 4850 – 4860; b) I. Weissbuch, P. N. W. Baxter, I. Kuzmenko, H. Cohen, S. Cohen, K. Kjaer, P. B. Howes, J. Als-Nielsen, J.-M. Lehn, L. Leiserowitz, M. Lahav, *Chem. Eur. J.* **2000**, *6*, 725 – 734.
[13] a) M. Haga, N. Kato, H. Monjushiro, K. Z. Wang, M. D. Hossain, *Supramol. Sci.* **1998**, *5*, 337 – 342; b) W. Y. Lee, M. Majda, G. Brezesinski, M. Wittek, D. Möbius, *J. Phys. Chem. B* **1999**, *103*, 6950 – 6956.
[14] a) J. Nagel, U. Oertel, *Thin Solid Films* **1998**, *329*, 495 – 498; b) J. Nagel, U. Oertel, P. Friedel, H. Komber, D. Möbius, *Langmuir* **1997**, *13*, 4693 – 4698; c) U. Oertel, J. Nagel, *Thin Solid Films* **1996**, *285*, 313 – 316.
[15] Y. Lvov, F. Essler, G. Decher, *J. Phys. Chem.* **1993**, *97*, 13773 – 13777.
[16] C. Erdelen, A. Laschewsky, H. Ringsdorf, J. Schneider, A. Schuster, *Thin Solid Films* **1989**, *180*, 153 – 166.
[17] K. de Meijere, G. Brezesinski, H. Möhwald, *Macromolecules* **1997**, *30*, 2337 – 2342.
[18] K. de Meijere, G. Brezesinski, K. Kjaer, H. Möhwald, *Langmuir* **1998**, *14*, 4204 – 4209.
[19] J. Engelking, M. Wittemann, M. Rehahn, H. Menzel, *Langmuir* **2000**, *16*, 3407 – 3413.
[20] E. C. Constable, *Adv. Inorg. Chem. Radiochem.* **1986**, *30*, 69 – 121.
[21] M. Antonietti, A. Kaul, A. Thünemann, *Langmuir* **1995**, *11*, 2633 – 2638.
[22] Repeated determination of the composition of PAC (**2**) yielded a ratio of six amphiphiles per MEPE repeating unit rather than 6 – 7 as published previously.
[23] P. Laine, A. Gourdon, J.-P. Launay, *Inorg. Chem.* **1995**, *34*, 5156 – 5156.
[24] In BAM, only a narrow strip of the image is in focus, because the surface is imaged under the Brewster angle. Therefore, objects that are outside the focus strip appear larger due to defocusing.
[25] The film area sampled by the X-ray probe beam exceeds several mm$^2$. Therefore, XRR measurements represent an average film structure.
[26] The volume of a MEPE (**1**) repeating unit was calculated as follows: 1.8 nm$^2$ (area) × 0.33 nm (thickness of π system) = 0.6 nm$^3$; the volume of box **a** is 1.7 nm$^3$ (1.9 nm$^2$ × 0.9 nm). Therefore, the occupied volume fraction of MEPE (**1**) is 35 %.
[27] A partial reorganization at the air/water interface was also observed in case of poly(propylene imine) dendrimers covalently modified with long hydrocarbon chains (A. P. H. J. Schenning, C. Elissenroman, J. W. Weener, M. W. P. L. Baars, S. J. Vandergaast, E. W. Meijer, *J. Am. Chem. Soc.* **1998**, *120*, 8199 – 8208).
[28] K. Kjaer, J. Majewski, H. Schulte-Schrepping, J. Weigelt, *HASYLAB Annu. Rep.* **1992**, 589 – 590.
[29] A. Asmussen, H. Riegler, *J. Chem. Phys.* **1996**, *104*, 8159 – 8164.
[30] J. Als-Nielsen, D. Jacquemain, K. Kjaer, F. Leveiller, M. Lahav, L. Leiserowitz, *Phys. Rep.* **1994**, *246*, 251 – 313.
[31] K. Kjaer, *Physica B* **1994**, *198*, 100 – 109.

Received: July 24, 2000
Revised version: November 13, 2000 [F2617]